Kinetics of Liposome Adhesion on a Mercury Electrode

Dirk Hellberg,[†] Fritz Scholz,*[,†] Frank Schubert,[‡] Milivoj Lovrić,[§] Dario Omanović,[§] Víctor Agmo Hernández,[†] and Richard Thede[†]

Institut für Chemie und Biochemie, Universität Greifswald, Greifswald, Germany, Lipoid GmbH, Ludwigshafen, Germany, and Rudjer Boskovic Institute, Zagreb, Croatia.

Received: February 16, 2005; In Final Form: June 2, 2005

The adhesion of liposomes on a mercury electrode leads to capacitive signals due to the formation of islands of lecithin monolayers. Integration of the current−time transients gives charge−time transients that can be fitted by the empirical equation $Q(t) = Q_0 + Q_1(1 - \exp(-t/\tau_1)) + Q_2(1 - \exp(-t/\tau_2))$, where the first term on the right side is caused by the docking of the liposome on the mercury surface, the second term is caused by the opening of the liposome, and the third term is caused by the spreading of the lecithin island on the mercury surface. The temperature dependence of the two time constants τ_1 and τ_2 and the temperature dependence of the overall adhesion rate allow determination of the activation energies of the opening, the spreading, and the overall adhesion process both for gel-phase 1,2-dimyristoyl-*sn*-glycero-3-phosphocholine (DMPC) and for liquid-crystalline-phase DMPC liposomes. In all cases, the spreading is the rate-determining process. Negative apparent activation energies for the spreading and overall adhesion process of liquid-crystalline-phase DMPC liposomes can be explained by taking into account the weak adsorption equilibria of the intact liposomes and the opened but not yet spread liposomes. A formal kinetic analysis of the reaction scheme supports the empirical equation used for fitting the charge−time transients. The developed kinetic model of liposome adhesion on mercury is similar to kinetic models published earlier to describe the fusion of liposomes. The new approach can be used to probe the stability of liposome membranes.

Introduction

The unique properties of liposomes have triggered numerous applications in various fields of science and technology, from basic studies of the shape of cells, mechanisms of membrane and membrane protein function, chemical catalysis, to applications such as drug delivery systems, medical diagnostics, transfection vectors, water-based ointments and gels in cosmetics, and self-healing paints. Phosphatidylcholines (lecithins) are the most widely used lipids in liposome work. They are zwitterionic at all physiological values of pH because of the quarternary ammonium group.

The lipid composition of biological membranes varies and depends on the tissue or organelles. In the case of bacterial membranes, the composition depends on their growth temperature.[1] Lipid membranes consisting of lecithins undergo different phase transitions depending on the temperature. It is the order−disorder display that is of biological relevance, and membranes consisting of extracted biological lipids have melting points close or not too far away from physiological temperature. The low-temperature lipid phase has hydrocarbon chains predominantly ordered in an all-trans configuration and is called the gel phase. The high-temperature phase is characterized by unordered chains and is called the liquid-crystalline or fluid phase. Unsaturated lecithins display significantly lower phase transition temperatures than saturated lipids. The phase transition temperatures (PTT) of lecithins in liposomes have been carefully determined and studied by several techniques, e.g., calorimetric measurements. Heerklotz and Seelig have used pressure perturbation calorimetry to measure the heat consumed or released by a liposomal suspension following a sudden pressure jump.[2] They have derived the volume changes of the pretransition and main transition of DMPC in multilamellar vesicles (MLVs), small unilamellar vesicles (SUVs) with an average diameter of 30 nm, and large unilamellar vesicles (LUVs) with an average diameter of 100 nm. Heimburg and co-workers have investigated MLVs close to the PTT by pressure-jump calorimetry.[3,4] The relaxation times that they have found are proportional to the heat capacity, which allows calculation of the PTT. Both groups have obtained a PTT of about 23.6 °C for DMPC liposomes, which coincides with that of bulk DMPC. Pouligny and co-workers have studied single DMPC vesicles with respect to their pretransitional effects by optical dynamometry.[5] Bagatolli and Gratton have visualized the phase transition of lecithins in giant unilamellar vesicles (GUV) by two-photon excitation fluorescence.[6−10] At temperatures very close to the main PTT ($\sim T_{PTT}$ − 1 °C), a movement of the whole vesicle has been observed. At the main PTT, the gel and the liquid-crystalline phases coexist, and the vesicle diameter increases. During the gel to liquid-crystalline phase transition, the shape of the liposome changes from spherical to polygonal. When the temperature is increased, the polygonal shape disappears, and the liposome assumes an ellipsoidal shape. In liposomes consisting of mixed lecithins, coexistence of the liquid-crystalline and the gel phases can be observed at temperatures between the different PTTs of the lecithins used (lipid domains coexisting). Hence, this method allows correlation of the microscopic organization on the surface of single vesicles with the physical parameters determined at a molecular level on the lipid bilayer membrane such as lipid mobility or lipid hydration. The intrinsic differences between the structures of GUVs and MLVs lead to a broadening of the phase transition in GUVs. Brumm et al. have shown that the

* Author to whom correspondence should be addressed. E-mail: fscholz@uni-greifswald.de.
[†] Universität Greifswald.
[‡] Lipoid GmbH.
[§] Rudjer Boskovic Institute.

10.1021/jp050816s CCC: $30.25
Published on Web 07/13/2005

highest PTT is reached in planar membranes.[11] The increase in the membrane curvature lowered the lateral pressure of the lipid membrane, which leads to a temperature shift. The pioneering work in electrochemical characterization of monolayers adsorbed on a mercury electrode was performed by Miller.[12−18] Lecithin monolayers adsorbed on the surface of a mercury electrode became fundamental for understanding biological membrane functions and are an alternative to free-standing artificial systems. The hydrocarbon tails of the lipid molecules are arranged on the hydrophobic mercury surface, and the hydrophilic lipid heads are directed into the electrolyte solution. One advantage is that the electric potential and the flux of electroreducible metal ions across the monolayer can be controlled more accurately and more directly than at bilayer lipid membranes. Another advantage is that the mechanical stability and a resistance to high electric fields are higher than those of bilayer lipid membranes.

The permeability of pure and protein-incorporated phospholipid monolayers at the mercury−water interface for faradaic reactions has been also extensively studied by Nelson and co-workers;[19−23] the adsorption of electroactive compounds such as safarin-T has been investigated by Guidelli and his group.[24−27] All produced the adsorbed monolayer by lowering a hanging mercury drop electrode (HMDE) very slowly through a phospholipid monolayer at the gas−solution (GS) interface. By measuring the differential capacity of the lipid film, they could show that near to the point of zero charge (pzc), e.g., between −0.2 and −0.7 V (vs Ag/AgCl), the capacity of the lipid film has a minimum value. That indicates a nonpermeable monolayer. At more negative and positive potentials, an increase of the capacity indicated that the monolayer became defective and therefore permeable. In the case of potassium-ion-containing electrolytes, the phospholipids desorb from the mercury at potentials more negative than −1.6 V (vs Ag/AgCl), because the electrostatic interaction between the charged mercury surface and the ions and dipoles of the solution is getting much stronger than the adsorption of the lipids. In lithium-ion-containing electrolytes, the desporption can be shifted toward even lower potentials as Guidelli et al. have shown.[26] Bizzotto and co-workers have shown that monolayers produced by layer adsorption from the GS interface exhibit a different behavior in alternating current (ac) voltammetric measurements than those produced by liposome adhesion from the solution.[28] The reason is the interaction of the defective monolayer at very negative potentials with liposomes in the suspension, which modifies the monolayer. These potential-induced changes of the monolayer were visualized in ac voltammetric measurements combined with in situ fluorescence microscopy[29,30] and were in good agreement with chronocoulometric charge density measurements published by Bizzotto and Nelson.[31]

The detection of single adhesion events by chronoamperometry was described for the first time by Žutić, Svetličić, and co-workers in the case of oil droplets and the unicellular algae *Dunaliella tertiolecta*.[32−37] They have demonstrated the potential depending on wetting and spreading of oil droplets. In our previous work, we discovered that it is also possible to detect the adhesion of single liposomes and montmorillonite particles on the surface of a mercury drop electrode by chronoamperometry.[38,39] The adhesion process leads to capacitive currents and results in the case of liposomes in an adsorbed lecithin monolayer on the mercury surface. The detection of liposome adhesion is an additional option to characterize liposomes, e.g., calculating the number of molecules per liposome. In the present work, we will describe a modified model of liposome adhesion and the results of a kinetic analysis of the adhesion process that can be understood on the basis of three basic steps of interaction: first, the contact making or docking of the intact liposome with the mercury surface, second, the opening of the attached liposome, and third, the spreading of the liposome and formation of an adsorbed monolayer island of lecithin molecules on the mercury surface. Analyzing the temperature dependence of the adhesion kinetics provides insight into the energetic pathway of the reaction sequence. Very recently, Lipkowski et al. described the adhesion kinetics of liposomes on the solution−air interface.[40] For temperatures above the PTT, their kinetic data indicate that the monolayer formation involves a fast rupture of a constant number of vesicles and the formation of disk-shaped monolayer islands at the air−solution interface. These islands grow with a constant radial rate. At higher coverages, the growth is limited by the overlap of the growth centers.

Materials and Methods

The pure phosphatidylcholines 1,2-dimyristoyl-*sn*-glycero-3-phosphocholine (DMPC), 1,2-dipalmitoyl-*sn*-glycero-3-phosphocholine (DPPC), and 1,2-dioleoyl-*sn*-glycero-3-phosphocholine (DOPC) from Lipoid GmbH, Ludwigshafen, Germany, have been studied and were used without further purification. Liposomal suspensions were prepared with 0.1 M KCl solution by thin film hydration and homogenized by extrusion with a microporous filter (450 nm) if not described otherwise. The mean diameter of the liposomes was in the range of 450 nm, and the concentration of lecithin in the suspension was 0.1 g L^{-1} (0.127−0.148 mM). The distribution of liposome diameters was controlled by light-scattering measurements with a Zetasizer 3000 HS (Malvern Instruments, Herrenberg, Germany). The measurements showed indeed a maximum at 450 nm for the samples homogenized by extrusion through a 450 nm filter, and they showed two maxima, one at 350 nm and one at 1800 nm, for the nonhomogenized samples. For charge density measurements, the liposomes were prepared by ultrasonication to get smaller vesicles and thus also a higher coverage of the electrode surface. In this case, the concentration of lecithin was between 0.015 and 0.02 mM. The electrolyte potassium chloride Suprapur was obtained from Merck, Darmstadt, Germany. The water used was prepared from deionized water by distilling it once with an addition of alkaline permanganate solution to oxidize traces of organic compounds, followed by another distillation. Before being measured, the suspensions were deaereted 20 min with high-purity nitrogen gas.

All electrochemical measurements were performed with an Autolab PSTAT 10 (Eco Chemie, Utrecht, Netherlands) interfaced to a P4 PC in conjunction with an electrode stand VA 663 (Methrom, Herisau, Switzerland). A multimode electrode was used as the working electrode, a platinum rod served as the auxiliary electrode, and an Ag|AgCl (3 M KCl, $E = 0.208$ V vs SHE) electrode was used as the reference electrode. The surface area of the mercury drop was 0.48 mm^2, as determined by weighing 50 drops.

The interaction of the liposomes with the electrode surface was recorded in chronoamperometric measurements performed within 1 s with sampling each 50 μs. The pzc was determined by sampled direct current (dc) polarography in a blank 0.1 M KCl solution. The determination of the surface charge densities of the lecithin-covered electrode was based on the work of Guidelli et al.[25] To calculate the charge density of the blank (for reasons of briefness, this term will be used here and later for the mercury−aqueous electrolyte interface) and the lecithin-covered mercury surface, double-step chronoamperometry was used. The investigated potential range was between 0 and −1.8 V. In the case of the blank surface, the potential was kept

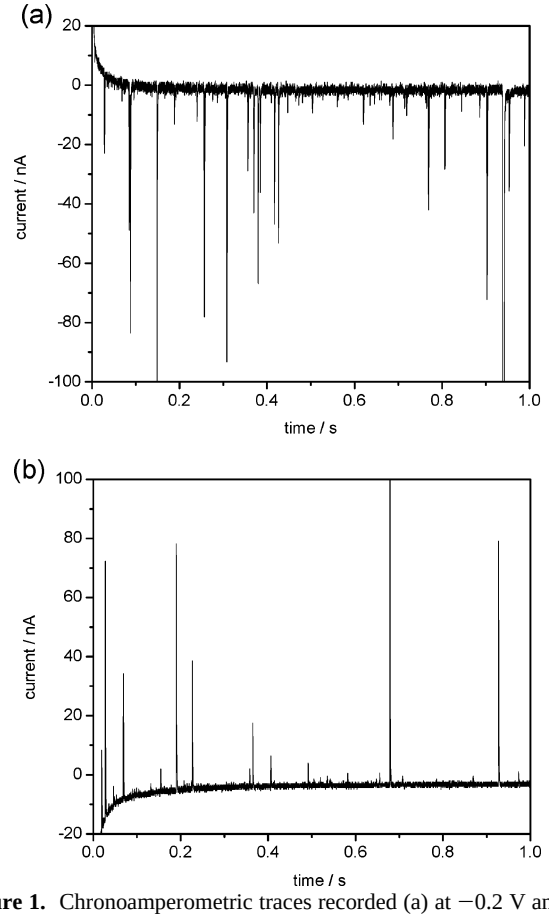

Figure 1. Chronoamperometric traces recorded (a) at −0.2 V and (b) at −0.7 V, the point of zero charge. The nonhomogenized suspension of DMPC liposomes was deaereted for 20 min by pure nitrogen, and the concentration of DMPC was 0.1 g L^{-1} in 0.1 M KCl solution.

constant for 15 ms in a 0.1 M KCl solution at the pzc and then pulsed for 50 ms to a potential at which the charge density had to be determined. The absolute charge density is the ratio of the charge of the resulting peak and the surface area of the drop. The determination of the lecithin-covered electrode surface is more complicated, and it was similar to the work of Bizzotto and Nelson.[32] A liposomal suspension was stirred for 100 s at an initial potential of −0.4 V to ensure a totally covered electrode surface. After the suspension was stirred, the potential was stepped for 15 ms to a value between 0 and −1.7 V. Then the potential was pulsed for 15 ms to −1.8 V. At this potential, the lecithin monolayer desorbs from the surface of the mercury drop. The ratio of the charge resulting from the potential step and the electrode surface area gives a charge density that has to be subtracted from the charge density at −1.8 V. The potential window of investigation is limited in the anodic direction by the oxidation of mercury, e.g., the reaction of mercury to calomel, and it is limited in the cathodic direction by the reduction of potassium and protons.

For counting and analysis of the adhesion peaks, the *Signal Counter* software was used.[41]

Results and Discussion

Capacitive Signals of Liposome Adhesion on a Mercury Drop Electrode. During the bursting and spreading process of liposomes on the surface of a static mercury drop electrode (SMDE), the lecithin molecules displace charge due to the displacement of water dipoles and ions from the solution side of the electrochemical double layer. This leads to a decrease of double-layer capacity. Hence, in chronoamperometric measurements under potentiostatic conditions, a capacitive current flows to equilibrate the system. This can be observed as a current peak in the chronoamperometric curves, provided that the charge displaced by a single liposome is large enough to be detectable. Figure 1 shows two typical chronoamperometric traces (a) above and (b) below the pzc recorded in a nonhomogenized liposomal suspension with 0.1 M KCl and 0.1 g L^{-1} DMPC at 25 °C. Above the pzc, the peaks have a negative sign because the lecithin molecules displace negative charges and electrons have to flow into the mercury to diminish the positive charge on the metal side. Below the pzc, the peaks have a positive sign because the displaced charge is positive, and therefore electrons have to leave the mercury to diminish the negative charge of the metal.

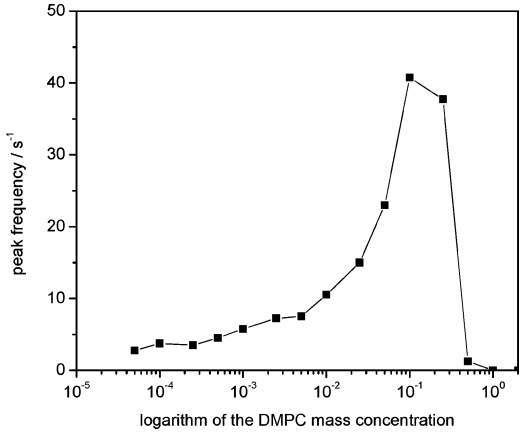

Figure 2. Dependence of the peak frequency on the DMPC concentration. The measurements were performed in a liposomal phosphate buffered saline solution, homogenized by filter extrusion (450 nm), at −0.2 V (vs 3 M Ag/AgCl) and 25 °C.

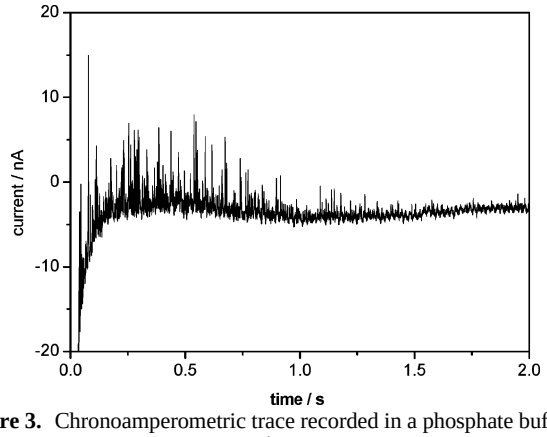

Figure 3. Chronoamperometric trace recorded in a phosphate buffered saline solution including 0.25 g L^{-1} nonhomogenized DMPC liposomes at 25 °C and −0.6 V.

The dependence of the peak frequency on the lecithin concentration is shown in Figure 2. First, the peak frequency increases linearly with the lecithin concentration. At 0.1 g L^{-1} the peak frequency reaches its maximum. Above this concentration, the peak frequency decreases because the number of liposome adhered is so high that the electrode gets completely covered within the time span of the measurement (cf. Figure 3). At 1 g L^{-1}, no capacitive peaks are observed anymore because the electrode is already getting fully covered during the formation of the new mercury drop and thus before the measurement starts. To ensure that the adhesion events occur on a clean mercury surface only, the concentration of liposomes was generally kept at a rather low level of 0.1 g L^{-1} of lecithin.

Figure 4 shows the dependence of the peak frequency on the potential in the case of DMPC liposomes in a 0.1 M KCl

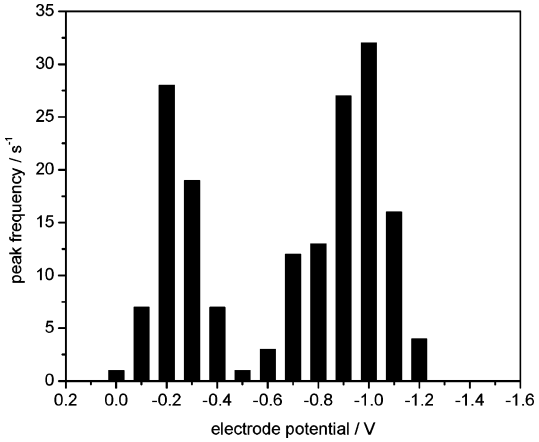

Figure 4. Dependence of the peak frequency on the electrode potential at 25 °C. The measurements were performed in a 0.1 M KCl solution including 0.1 g L^{-1} DMPC liposomes, homogenized by filter extrusion (450 nm).

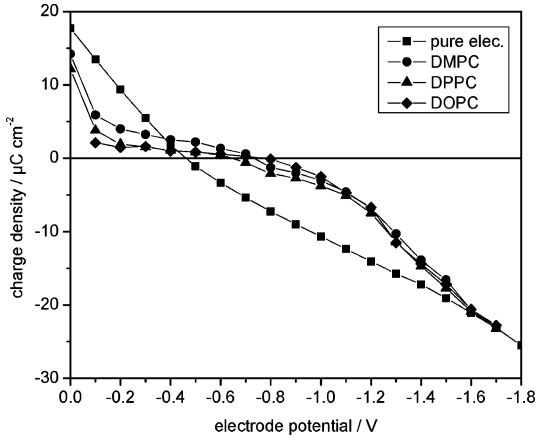

Figure 5. Charge densities of a blank static mercury drop electrode (squares) and a static mercury drop electrode fully covered with a DMPC (circles), DPPC (triangles), and DOPC monolayer (diamonds) at different potentials vs 3 M Ag/AgCl and 25 °C. The monolayers were produced by liposome adhesion.

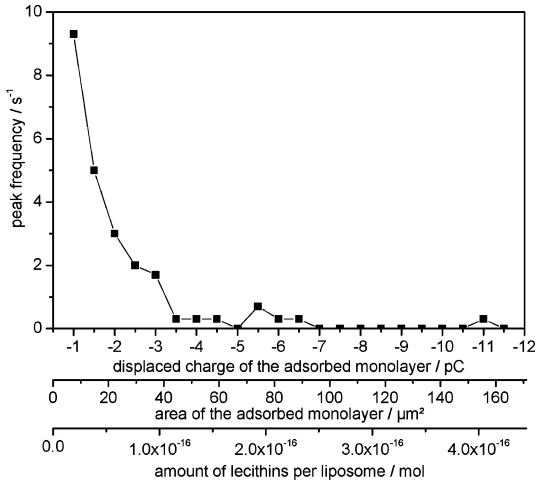

Figure 6. Distribution of the peak frequency of a suspension of DMPC liposomes, homogenized by filter extrusion (450 nm), dependence on the displaced charge of the adsorbed monolayer, the area of the adsorbed monolayer, and the number of lecithin molecules per liposome investigated at −0.9 V and 25 °C. The concentration of DMPC was 0.1 g L^{-1} suspended in 0.1 M KCl solution.

solution at 25 °C. The peak frequency has a minimum at −0.5 V, which was the measuring potential next to the pzc. The more negative and positive the applied potential is relative to the pzc, the more the peak frequency increases. The maximum values are reached at −0.2 and −1.0 V. For potentials positive to −0.2 V and negative to −1.0 V, the peak frequency decreases until no peaks could be observed at potentials positive to 0.0 V and negative to −1.2 V.

The peak frequencies in the potential range from −0.2 to −1.1 V do not represent the absolute but just the *detectable* number of liposome adhesions per second. At the pzc, the electrochemical double layer does not possess any extra charge on the two sides of the interface. However, to produce a capacitive current that can be recorded in a current−time curve, a liposome has to displace a minimum value of charge. Therefore, adhesion of liposomes at the pzc cannot be observed. Above and below the pzc, the charge density is increasing, of course, with opposite signs. However, at low charge densities, only the largest liposomes displace a charge that is detectable. The higher the charge density of the electrode, the higher will be the peak frequency because more and more of the smaller liposomes are detectable. Although in our measurements we could identify peaks with a charge of 0.1 pC, the signal-to-noise ratio of those peaks was too low for detailed studies. Therefore, we used for evaluations only peaks of a charge above 1 pC. At −1.0 V, the sensitivity of lipsosome detection, i.e., the number of adhesion events per time, reaches its maximum. This is the case because at potentials toward the pzc the amount of displaced charge per lecithin molecule decreases and leaves only the largest liposomes to be detectable. The decrease of the peak frequency above −0.1 V and below −1.1 V can be explained as follows: The interaction of the lecithin molecules and the mercury drop relies on the hydrophobic properties of the lipophilic tail of the lecithin and the mercury. When the potential is shifted to very positive or negative values, relative to the pzc, the effect of the polarity of the mercury drop becomes stronger than its hydrophobic forces. At these potentials, an anchoring of liposomes by adsorption of some lecithin molecules of the liposome becomes very unfavorable. Parallel to the decrease of the peak frequency, the peak size decreases too, and the shape deteriorates. Peaks at −1.2 V are very broad in relation to those at potentials between −0.2 and −1.0 V. At potentials negative to −1.2 V, no peaks could be observed. Bizzotto and co-workers have proposed for the potential range −1.2 to −1.6 V that the interaction between liposomes and the mercury leads to the adhesion of liposomes as small spheres on the surface.[29] This proposal is in agreement with the work of Nelson and Bizzotto when they have described potential-induced phase transitions of lecithin monolayers adsorbed on a hanging mercury drop electrode.[32] Our comparison of the charge densities of a noncovered SMDE and a SMDE covered by different lecithin monolayers such as DMPC, DPPC, and DOPC in dependence on the potential (Figure 5) is generally in agreement with their work. Very interestingly, we have observed peaks that have the shape of the first derivative of a peak, i.e., with a positive maximum and a negative minimum, at potentials of −1.2, −0.5, and −0.8 V. However, these peaks have been observed only occasionally, and we could not find out what conditions were responsible for their occurrence. We suppose that such events are due to reorganizations in the adsorbed layer of the opening and adhering liposomes. From the work of Bizotto et al., it is known that lecithin layers exist on mercury at potentials below −1.2 V. Thus, it is interesting that we could not observe the adhesion events at these potentials. Possible explanations are (i) that desorption of a previously formed adsorbed layer is kinetically hindered or (ii) that the repulsion of the outer side of liposomes is so strong at these potentials that the adhesion is prevented, although thermodynamically perhaps

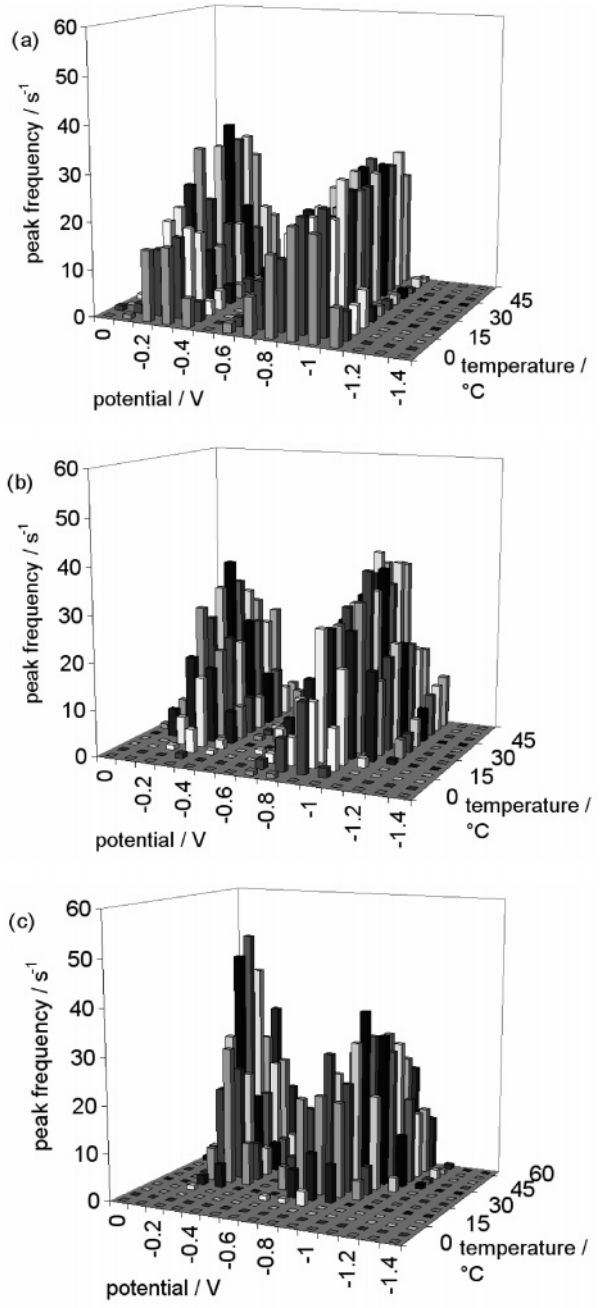

Figure 7. Peak frequency in dependence on the electrode potential and the temperature shown for (a) DOPC liposomes, (b) DMPC liposomes, and (c) DPPC liposomes. The measurements were performed in 0.1 M KCl solutions with 0.1 g L^{-1} DMPC, DPPC, or DOPC liposomes, homogenized by filter extrusion (450 nm).

allowed. The coverage of the mercury drop has been achieved by liposome adsorption at −0.4 V for 100 s. In the range between 0.0 and −1.6 V, the charge densities of the lecithin-coated SMDE are lower than those of the blank electrode. The potential-induced changes in the phase transition of the adsorbed monolayer reported by Nelson and Bizzotto are shown in the changes of the lecithin-coated charge density values. At potentials more negative than −1.6 V, the monolayers desorb, and therefore the charge densities of the electrodes become equal.

Calculation of the Sizes of the Lecithin Islands and the Number of Lecithin Molecules per Island, i.e., per Liposome, Formed by Adhesion of Liposomes. Integrating a capacitive current peak gives the charge displaced by one liposome. From the ratio of the displaced charge Q_{liposome} and the difference Δq of the charge densities for the interfaces mercury−solution and

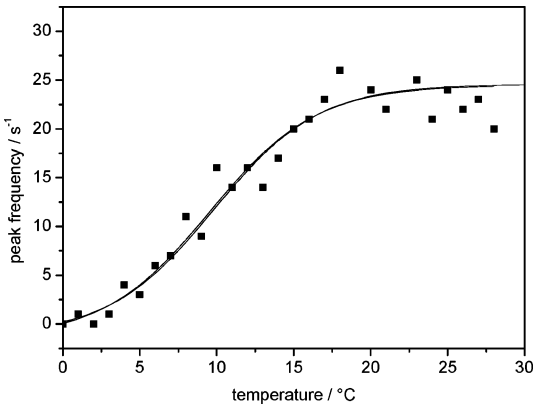

Figure 8. Peak frequency of DMPC liposomes dependence on the temperature at −0.9 V. The conditions are the same as in Figure 6.

mercury−lecithin−solution at the applied potential, the area of the adsorbed monolayer $A_{\text{monolayer}}$ on the mercury drop can be calculated

$$A_{\text{monolayer}} = \frac{Q_{\text{liposome}}}{\Delta q} \tag{1}$$

when A_{lecithin} is the area covered by one lecithin molecule,[42] the amount of moles of lecithin molecules in one liposome n_{lecithin} can be calculated as well

$$n_{\text{lecithin}} = \frac{A_{\text{monolayer}}}{A_{\text{lecithin}} N_{\text{A}}} \tag{2}$$

(N_{A} is the Avogadro constant.)

Figure 6 shows the distribution of peak frequencies versus displaced charges, covered areas, and moles of lecithin per liposome. For the smallest fraction of liposomes, the highest frequencies are observed. The capacitive peaks have been counted only for charges higher than 1 pC, which corresponds at −0.9 V to a monolayer area of 14.3 μm^2 and 3.7 × 10^{-17} mol lecithin per liposome. The capacitive peaks detected in liposomal suspensions of DMPC, DPPC, and DOPC, homogenized by filter extrusion (pore diameter 450 nm), were always in the range of 1−15 pC. For nonhomogenized suspensions, even larger charges were detected. In principle, one can calculate from the amount of lecithin per liposome its radius and volume; however, the results depend on the model, i.e., whether unilamellar or multilamellar liposomes are assumed. Assuming unilamellar liposomes, 1 pC would correspond to a liposome with a 1.5 μm diameter. When the liposome is completely filled with lecithin molecules, the same charge corresponds just to a liposome of 400 nm. Light-scattering measurements of the same suspensions showed a Gaussian distribution with a maximum at a diameter of 440 nm. From this, it can be concluded that the capacitive signals are caused by the fraction of the largest liposomes and those that are MLVs. At a potential of −0.9 V, a unilamellar DMPC vesicle with a diameter of 450 nm would displace an amount of charge of about 0.09 pC, which is one-tenth of what can be detected.

Figure 7 depicts for all three lecithins three-dimensional plots of the peak frequencies as functions of potential and temperature. These plots show only the general trends, because they are rather noisy due to the limited number of possible measurements for each potential−temperature coordinate. For each coordinate, three measurements have been performed; however, for the entire grid this means that about 13 740 peaks had to be evaluated. Clearly, it was impossible to increase the number of

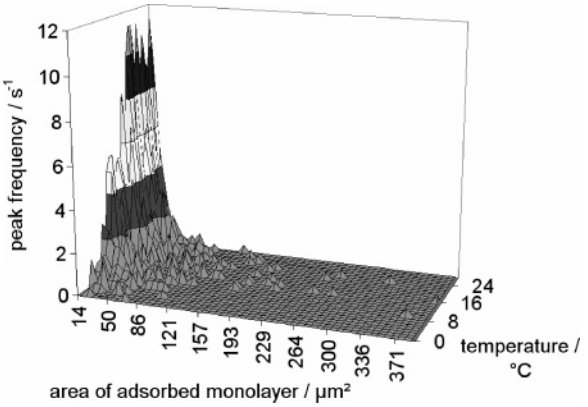

Figure 9. Distribution of the peak frequency of DMPC liposomes dependence on the area of an adsorbed monolayer and the temperature at −0.9 V. The conditions are the same as in Figure 6.

samplings by a factor of 10 or so to sufficiently improve the signal-to-noise ratio. Therefore, only for a small number of well-chosen coordinates, more detailed plots have been constructed. Nevertheless, Figure 7 shows that adhesion processes can be detected well below the PTT. Adhesion of DMPC liposomes begins at lower temperatures than adhesion of DPPC liposomes because the PTT of DMPC (23.6 °C) is lower than that of DPPC (41.1 °C). In the case of DOPC liposomes (Figure 7a), the peak frequency is fairly constant over the entire studied temperature range because its PTT is about −18.0 °C. Figure 8 shows the peak frequency in dependence on the temperature for DMPC liposomes at −0.9 V in more detail, i.e., including many more measurements than in Figure 7 for the same potential. Even near to 0 °C, a few adhesions per second could be recorded, and the frequency increases up to about 20 °C where it eventually becomes roughly constant or only slightly decreasing. Figure 9, which shows a plot of the peak frequency versus temperature and the areas of islands of adsorbed lecithins, visualizes that the dependence depicted in Figure 8 is not dependent on the liposome size, i.e., the area of formed islands. The dependence shown in Figure 8, however, is strongly affected by temperature and potential. At certain potentials, first adhesion processes can be observed for DMPC and DPPC liposomes as much as 20 °C below the PTT. The plateau is reached in some cases for DPPC liposomes more than 15 °C below the PTT.

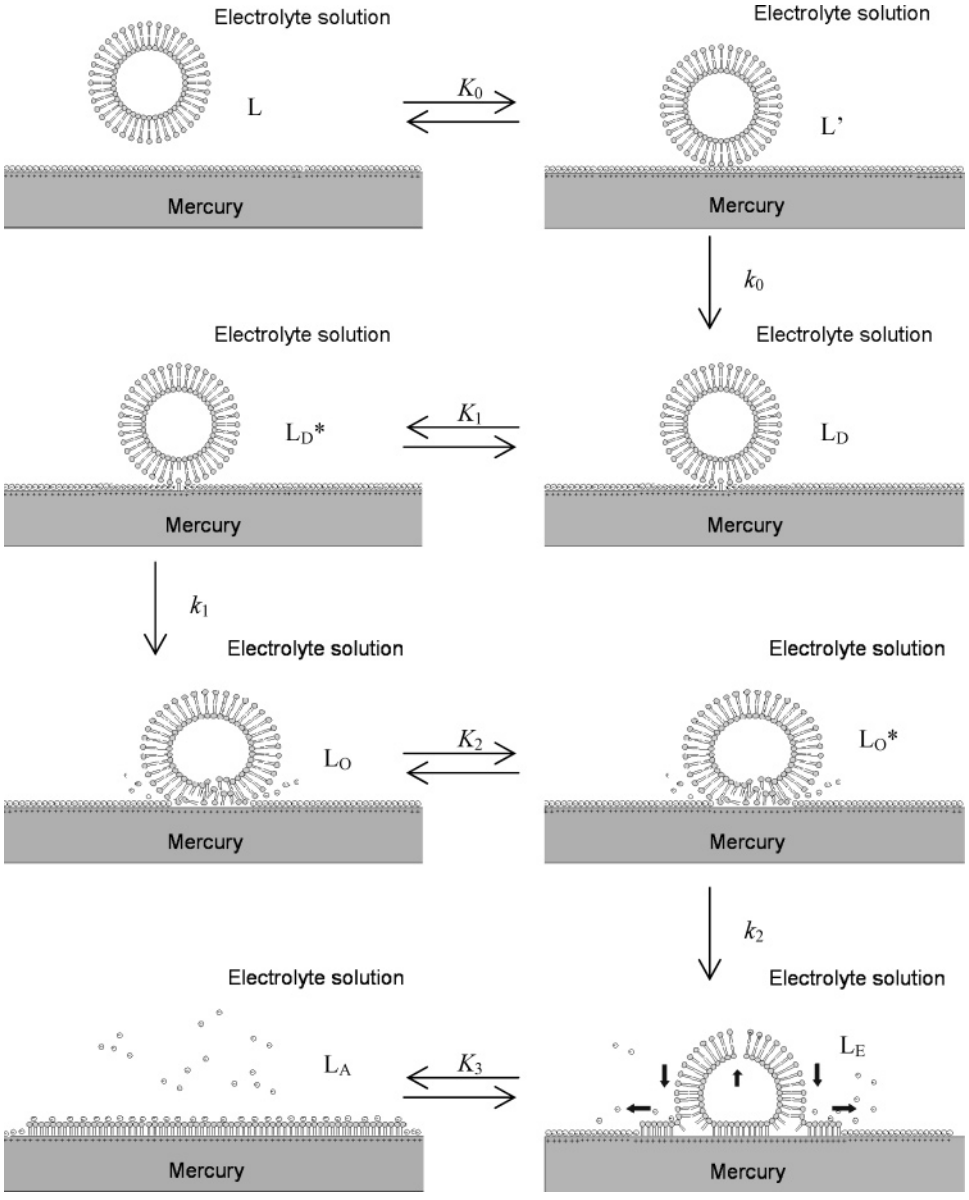

Figure 10. Proposed model of the adhesion process in the case of unilamellar liposomes. For explanation, see text.

The potential window in which adhesion is observed increases with increasing temperature, reaches its maximum close to the PTT, and becomes constant at higher temperatures. DOPC liposomes can be detected in the range from 0.0 to −1.1 V, DMPC and DPPC liposomes from 0.0 to −1.2 V. Peaks at −1.2 V were very broad and not suitable for any further investigations. This observation will be studied in detail in future work.

Adhesion Kinetics

When an intact suspended liposome adheres to a charged surface and spreads in the form of a layer of adsorbed lecithin molecules, this process must proceed in steps. In a very simple model, one may assume three steps. Later, we shall show that a more sophisticated model (Figure 10) is better suited to explain all the experimental data. As the first step, we assume that the liposome contacts the mercury surface with its outer polar surface, without being deformed. This is the so-called docking step. The second step will be an increasing deformation of the liposome along with an opening of the wall that allows some of the hydrophobic tails of the lecithin molecules to interact with the mercury surface. This stage we call the opening step. In the third step, the wall deconvolutes, and the lecithin molecules form a growing island of an adsorbed layer on the surface of the mercury. This stage is referred to as the spreading step. The model is based on the assumption that the lecithin molecules form a layer of adsorbed molecules that does not reorganize in one or the other way. Such a detailed feature may be studied in the future in more sophisticated models.

To extract kinetic information on these steps, it is mandatory that they are slower than the pure double-layer charging of the newly formed interface. Therefore, we determined the time constant τ of the charging of the electrochemical double layer of the blank and lipid-covered electrode by impedance measurements. The time constant is given by $\tau = RC$, where R is the specific resistance of the system and C is the specific capacity of the mercury−solution interface. The time constant of a blank mercury drop electrode at −0.7 V was about 8.4×10^{-3} s cm^{-2} and of a DMPC covered electrode about 3.5×10^{-3} s cm^{-2}. These values are near to those found by others.[43] The time constants of the adhesion process are, depending on the sizes of the liposomes, in the range of 1×10^{1} to 5×10^{3} s cm^{-2}; i.e., they were at least some orders of magnitude larger. (Here, the time constants of adhesion are given in units of s cm^{-2} to allow a comparison with the time constants of double-layer charging.)

To simulate the adhesion process, the current peaks of the adhesion events were integrated to provide charge versus time curves. On the basis of the described three-step model, we assumed that the first step, i.e., the docking, is so fast that we cannot resolve its time dependence. For the second and third steps, we have assumed that they follow a first-order kinetics, characterized by the time constants τ_1 and τ_2. Thus, the entire charge−time curve should follow the following equation

$$Q_{\text{monolayer}}(t) = Q_0 + Q_1(1 - \exp(-t/\tau_1)) + Q_2(1 - \exp(-t/\tau_1)) \quad (3)$$

The first term represents the docking step, the second one the opening, and the third term the spreading step. $Q_{\text{monolayer}}(t)$ is the total charge displaced by the adhesion of a single liposome. Q_0 is the charge displaced by the intact liposome when it contacts the electrode surface. Since the first step is too fast to be resolved in the reported measurements, there is no time dependence of that step taken into account in eq 3. Figure 11a shows a current peak, and Figure 11b the corresponding charge versus time curve together with the fitting curve based on eq 3.

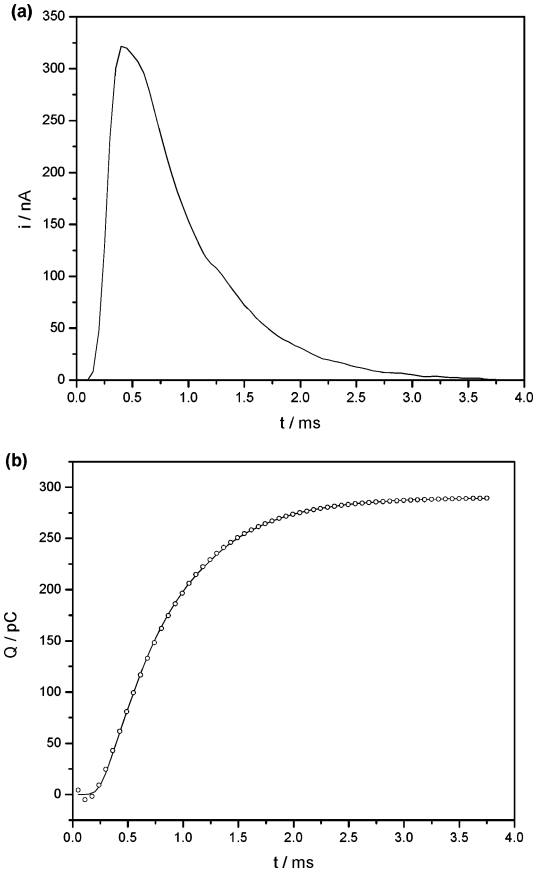

Figure 11. (a**)** Current−time curve showing an adhesion event of a DMPC liposome in a 0.1 M KCl solution with 0.1 g L^{-1} DMPC at −0.9 V and 28 °C and **(**b**)** fitting of an integrated capacitive peak caused by a DMPC liposome. The fitting was performed using eq 3: full line, experimental curve; open circles, fitted curve.

The quality of fitting was in almost all cases as good as that shown in the figure. When worse fittings have been obtained, the data were discarded, because, most probably, these peaks represented overlapping adhesion events. To quantitatively evaluate the goodness of fit, the chi-square-based probability Q was estimated.[44] Since the liposomes differ in size, the data series cannot be compared directly, and therefore the data series were reduced with respect to their global maximum. The reduced data series are fairly comparable, and from those two being most similar (otherwise the standard deviation could be overestimated leading to unreasonably large values of Q), the average relative standard deviation of the series was evaluated. The product from the relative average standard deviation and the global maximum of any of the data series should be some estimate for the average standard deviation of a single datum within a series, which would be observed by repeated measurement of the same liposome. The Q-probabilities estimated from these standard deviations and the chi-square values from the nonlinear regression are in any case larger than 0.001, in many cases even larger than 0.9; i.e., the fitting of the model to the data is reasonable. This is also supported by the coefficients of determination being always larger than 0.9.

Figures 12a−c show that the values Q_0, Q_1, and Q_2 depend on the overall charge $Q_{\text{monolayer}}$ displaced by a liposome; i.e., these values increase with increasing liposome size. The dependence of Q_0 on the liposome size is certainly less pronounced, because it is understandable based on the three-step model. The Q_0 values are also the smallest since the contact of the mercury surface by an intact liposome will only slightly change the double-layer capacity. The opposite signs of the Q_1 values in relation to those of Q_0 and Q_2 can be easily understood

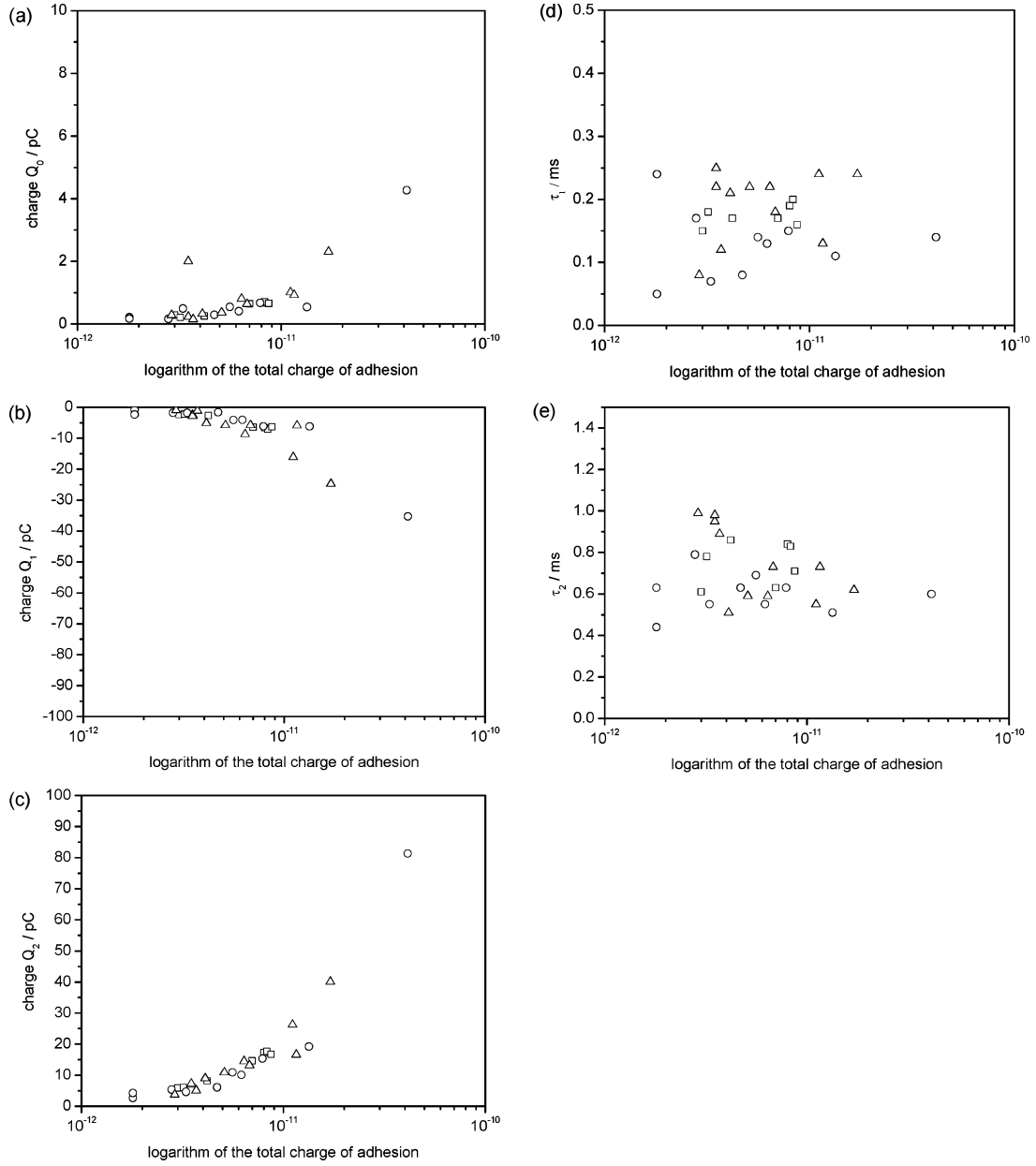

Figure 12. Dependence of (a) Q_0, (b) Q_1, (c) Q_2, (d) τ_1, and (e) τ_2 on the total charge of adhesion $Q_{\text{monolayer}}$ shown for three different potentials below the pzc: −0.6 V (squares), −0.8 V (circles), and −1.1 V (triangles). The investigated peaks were recorded in a 0.1M KCl solution with 0.1 g L^{-1} homogenized (450 nm, by pressure filtration) DMPC liposomes at −0.9 V and 28 °C.

as a pseudo-capacity caused by the rapid reconstruction of the interface between the opening liposome and the mercury surface, increasing temporarily the double-layer capacity. On the basis of the three-step model of adhesion, one would not expect a dependence of the time constants on the sizes of the liposomes. Indeed, that was not observed, although the data are rather scattered (Figures 12d and 12e). We suppose that the reason for the scattering of data is the morphological variation of the liposomes in our experiments (MLV, SUV, and LUV). The adhesion process of multilamellar liposomes is certainly more complex than that of unilamellar vesicles. Thus, each double layer of a MLV has to undergo an individual opening step. The time constants τ_1 and τ_2 show a slight dependence on the electrode potential (Figures 13a and 13b). Both time constants exhibit a minimum at the pzc, although this is less pronounced for the spreading process. The potential dependence of the time constants can be rationalized in terms of activation energies (see below) and double-layer structure, because the activation energies of the opening and the spreading will increase with the increasing charge of the double layer because this charge has to be removed upon lecithin adsorption.

A key experiment to understand the adhesion of liposomes is to study the dependence of adhesion frequency on time: If the entire process is limited by a diffusive transport of liposomes to the electrode surface, then a Cottrell-like dependence should be observed. This, however, is not the case as Figure 14 proves. This figure shows a plot of the frequency of adhesion events as a function of measuring time. Very clearly, the frequency does not decrease according to a $t^{-1/2}$ dependence, although a very small decrease may be present at long observation times. This is most probably the effect of an increasing surface coverage with islands of adsorbed lecithin layers, although this effect was minimized by using low liposome concentrations. The time independence of the frequency of adhesion events clearly proves that not each liposome that advances to the electrode surface is undergoing the adhesion process, but only a very small fraction of all the liposomes is successfully adhering. This can be understood when a rather large activation barrier has to be

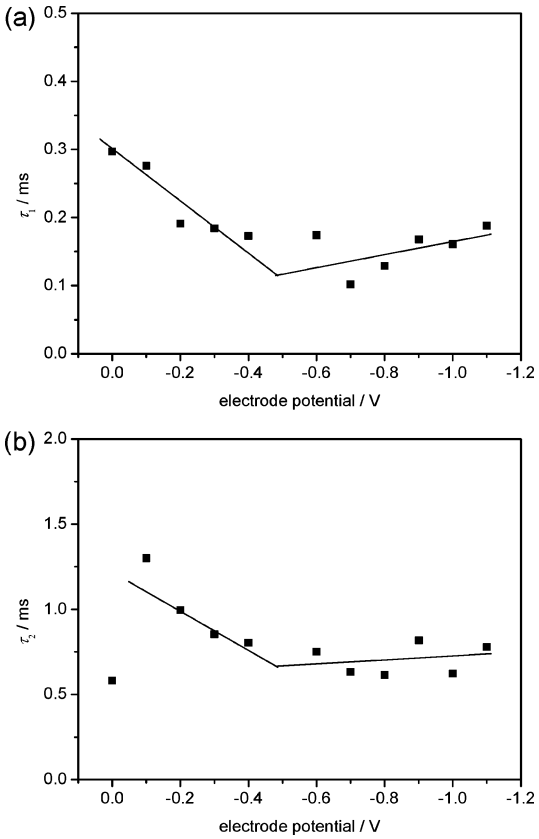

Figure 13. Time constants (a) of the opening step τ_1 and (b) the spreading step τ_2 dependence on the electrode potential. The peak frequency was recorded in a suspension of 0.1 g L^{-1} DMPC liposomes in 0.1 M KCl solution at 25 °C.

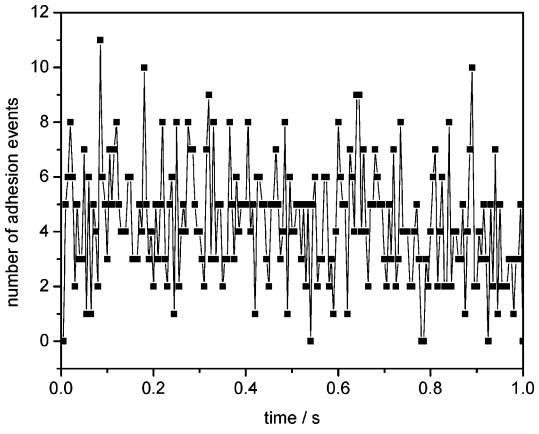

Figure 14. Number of adhesion events per 5 ms increments summed up over 50 independent measurements dependence on the time of measurement. The measurements were recorded in a suspension of 0.1 g L^{-1} DMPC liposomes in 0.1 M KCl solution at −0.9 V and 25 °C.

overcome for the adhesion. Therefore, we determined the activation energies of both the opening and the spreading processes in dependence on temperature at an electrode potential of −0.9 V. The constants Q_0, Q_1, and Q_2 of eq 3 depend on the total amount of charge $Q_{\text{monolayer}}$; however, they do not depend on the temperature. The time constants τ_1 and τ_2, however, depend on the temperature (Figure 15). With an increase in temperature, τ_1 decreases rather strongly until the PTT of DMPC (23.6 °C), and it decreases only very slightly above the PTT. The time constant τ_2 decreases with increasing temperature until the PTT and shows a very slight increase at temperatures above the PTT. The energies of activation were calculated applying the Arrhenius equation $k = A\ e^{-E_A/RT}$ and plotting ln k versus

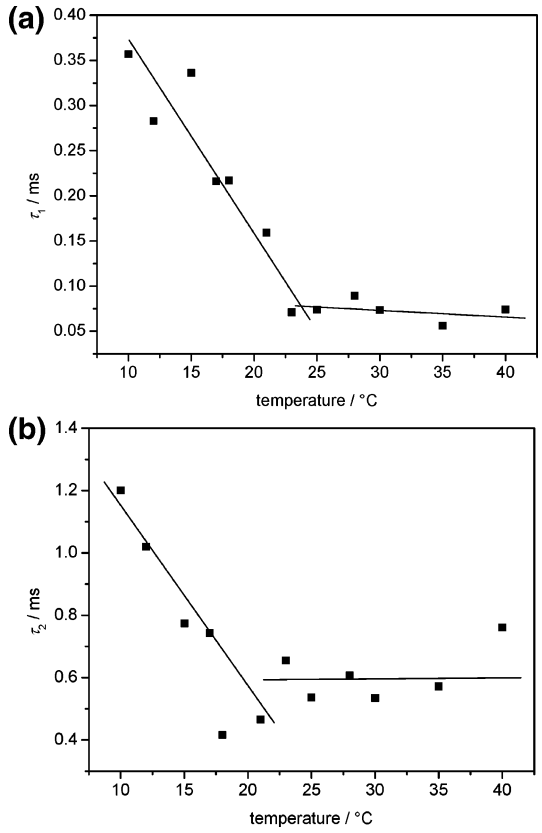

Figure 15. Time constants of DMPC liposome adhesion dependence on the temperature: (a) time constant τ_1 of the opening process and (b) time constant τ_2 of the spreading process. The conditions are the same as in Figure 6.

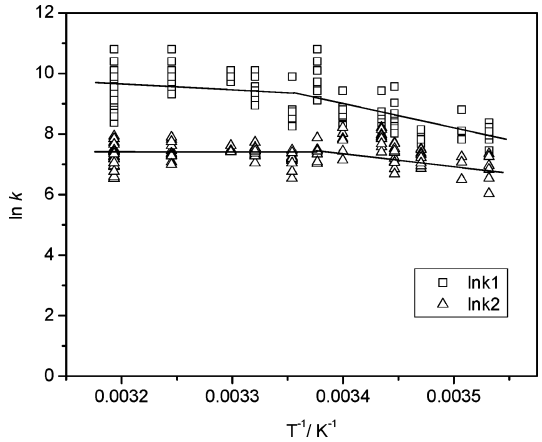

Figure 16. Plot of ln k as a function of T^{-1} for the opening (squares) and the spreading (triangles) process of DMPC liposomes. The values are calculated from the data displayed in Figure 15. The conditions of measurement are the same as in Figure 6.

the reciprocal temperatures. (See Figure 16 for the rate constants of the opening and the spreading processes.)

$$\ln k = \ln A - \frac{E_A}{RT}$$

The activation energy E_A of the opening process in the gel phase is 73 kJ mol^{-1}, and of the spreading process about 45 kJ mol^{-1}. The spreading is the rate-determining process as can be seen by the much larger time constants. The activation energy of the total adhesion process of liposomes existing in the gel phase can be calculated by taking the adhesion frequency as a

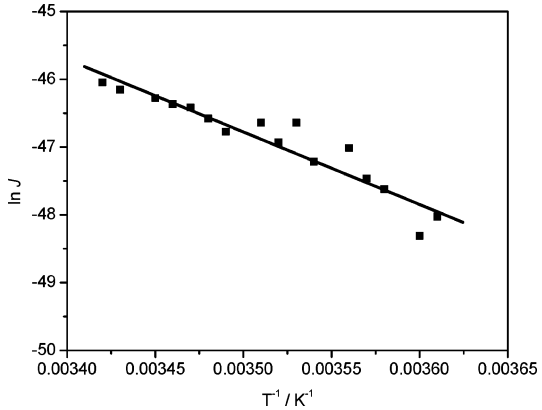

Figure 17. Plot of ln J as a function of T^{-1} for the total adhesion process in the case of DMPC liposomes at −0.9 V. The plot is based on the data shown in Figure 7.

measure of the adhesion rate and studying its dependence on temperature (Figure 8). Over the range from 4 to 19 °C, we calculated ln J, with J being the peak frequency f divided by the product of the surface area of the mercury drop A_{SMDE} and the Avogadro constant N_A

$$J = \frac{f}{A_{SMDE} N_A} \tag{4}$$

Plotting ln J versus reciprocal temperatures (Figure 17) yields an activation energy of 89 kJ mol^{-1} for the overall adhesion process of DMPC liposomes below the PTT, which is remarkably close to the value of the activation energy of the opening process.

For liquid-crystalline phase liposomes, the activation energy E_A of the opening process is about 9 kJ mol^{-1} (Figure 16), which is only one-fifth of the value in the gel phase. The activation energy of the spreading process is −15 kJ mol^{-1}, and the activation energy of the overall adhesion process is negative, −10 kJ mol^{-1}. These negative activation energies can be understood as apparent activation energies caused by the involvement of adsorption equilibria, in a way that the apparent rate constant is the product of a true rate constant and a equilibrium constant of adsorption. This becomes clear when one attempts an analysis of the formal kinetics of the system. To further corroborate the model, the following scheme has been developed

$$\mathrm{L} \overset{K_0}{\rightleftharpoons} \mathrm{L'} \overset{k_0}{\longrightarrow} \mathrm{L_D} \overset{K_1}{\rightleftharpoons} \mathrm{L_{D^*}} \overset{k_1}{\longrightarrow} \mathrm{L_O} \overset{K_2}{\rightleftharpoons} \mathrm{L_{O^*}} \overset{k_2}{\longrightarrow} \mathrm{L_E} \overset{K_3}{\rightleftharpoons} \mathrm{L_A} \tag{5}$$

L, free liposome

L′, liposome in contact with mercury surface

L_D, docked liposome ("one lecithin molecule adsorbed on mercury")

L_{D^*}, docked liposome in deformed state

L_O, opened liposome

L_{O^*}, adsorbed open liposome

L_E, "deconvoluted" liposome, i.e., lecithin island that is not yet adsorbed

L_A, island of adsorbed lecithin molecules

Figure 10 illustrates the reaction scheme in detail. At first, it has to be made clear that two very different kinetics have been studied here: The overall kinetics or *macroscopic kinetics*, i.e., the study of the rate of adhesion events, are based on the ensemble of liposomes suspended in a solution. These kinetics show practically no time dependence (cf. Figure 14), indicating that a very slow step is rate-limiting. The second kinetics are those of the single adhesion events, i.e., the *microscopic kinetics*. The kinetics of all the single adhesion events (the microscopic kinetics) are very reproducible and independent of the liposome concentration. These kinetics are related to the number of lecithin molecules in a single liposome being in the same state of configuration (one may treat that as a concentration of lecithin molecules in a liposome). There will be a specific way of altering the position within the liposome and adsorbing to the mercury surface for each of the lecithin molecules, which cannot be resolved. However, these complications are circumvented assuming a "lumped" model. The kinetics of single adhesion events are described by the sequence of equilibria and irreversible reactions written in eq 5. The first equilibrium (K_0) describes the very fast and rather weak adsorption of intact liposomes L producing L′, i.e., liposomes very loosely adsorbed on mercury. The capacitive measuring effect of that step will be very small because the liposomes have a rather polar outer surface that will only marginally alter the electrode charge at the contact surface. The next step is assumed to be a very slow irreversible reaction (k_0) in which one (or a few) lecithin molecules turn around and dock the liposome on the mercury surface forming L_D. The docked liposome L_D will adsorb in an equilibrium reaction (K_1) and produce L_{D^*}. The opening of L_{D^*} produces L_O, and this is a process that can be resolved in our measurements (k_1). This process has the time constant τ_1. In an equilibrium reaction, the opened liposome will form an *adsorbed* open liposome L_{O^*}. Now this adsorbed open liposome will spread in an irreversible reaction (k_2) to form an island of lecithin molecules that is strongly adsorbed. The latter can be described by adsorption equilibrium K_3. Of course, both processes, the spreading and the adsorption, are strongly coupled, but for a formal kinetic analysis they may be treated as two reaction steps. The thermodynamic equilibrium constants K_1, K_2, and K_3 can be understood as the ratios of the forward and backward reactions

$$K_i = \frac{k_{fi}}{k_{bi}} \tag{6}$$

With that definition the following equations can be written

$$\frac{d[L_D]}{dt} = -k_{f1}[L_D] + k_{b1}[L_{D^*}] \tag{7}$$

$$\frac{d[L_{D^*}]}{dt} = k_{f1}[L_D] - k_{b1}[L_{D^*}] - k_1[L_{D^*}] \tag{8}$$

$$\frac{d[L_O]}{dt} = k_1[L_{D^*}] - k_{f2}[L_O] + k_{b2}[L_{O^*}] \tag{9}$$

$$\frac{d[L_{O^*}]}{dt} = k_{f2}[L_O] - k_{b2}[L_{O^*}] - k_2[L_{O^*}] \tag{10}$$

$$\frac{d[L_E]}{dt} = k_2[L_{O^*}] - k_{f3}[L_E] + k_{b3}[L_A] \tag{11}$$

$$\frac{d[L_A]}{dt} = k_{f3}[L_E] - k_{b3}[L_A] \tag{12}$$

Pairwise addition of the equations gives

$$\frac{d[L_D]}{dt} + \frac{d[L_{D^*}]}{dt} = -k_1[L_{D^*}] \tag{13}$$

$$\frac{d[L_O]}{dt} + \frac{d[L_{O^*}]}{dt} = k_1[L_{D^*}] - k_2[L_{O^*}] \tag{14}$$

$$\frac{d[L_E]}{dt} + \frac{d[L_A]}{dt} = k_2[L_{O^*}] \tag{15}$$

By incorporation of the equilibria, the following equations can be derived

$$(1 + K_1)\frac{d[L_{D^*}]}{dt} = -k_1K_1[L_D] \quad (16)$$

$$(1 + K_2)\frac{d[L_O]}{dt} = -k_1K_1[L_D] - k_2K_2[L_O] \quad (17)$$

$$(1 + K_3)\frac{d[L_E]}{dt} = k_2K_2[L_O] \quad (18)$$

$$[L_{D^*}] = K_1[L_D] \quad (19)$$

$$[L_{O^*}] = K_2[L_O] \quad (20)$$

$$[L_A] = K_3[L_E] \quad (21)$$

Taking into account appropriate response factors, addition of all liposome species yields the final equation

$$Y = A_0 + A_1\left(1 - \exp\left(-\frac{t}{\frac{1 + K_1}{k_1K_1}}\right)\right) + A_2\left(1 - \exp\left(-\frac{t}{\frac{1 + K_2}{k_2K_2}}\right)\right) \quad (22)$$

Comparing eq 22 with the empirical eq 3 used for fitting the charge transients reveals the meaning of the time constants τ_1 and τ_2

$$\tau_1 = \frac{1 + K_1}{k_1K_1} \quad (23)$$

$$\tau_2 = \frac{1 + K_2}{k_2K_2} \quad (24)$$

The thermodynamic equilibrium constants of adsorption decrease with increasing temperature. When K_1 and K_2 are smaller than 1 at higher temperatures, apparent negative activation energies are possible, whereas for lower temperatures they may be larger than 1, which may lead to the result that they cancel in eqs 23 and 24 and thus allow the observation of positive activation energies.

The rate constant of the overall kinetics of adhesion events follows from the scheme in eq 5 as the product of K_0 and k_0. The docking step with the very small k_0 is the bottleneck of the overall adhesion kinetics (macroscopic kinetics, looking at all the liposomes). The adsorption equilibrium K_0 affects the overall rate in such way that for temperatures above the PTT even negative apparent activation energies are measured.

Eventually, it needs to be said that the reactions transforming L_D into L_A can also be formulated as follows

$$L \overset{K_0}{\rightleftharpoons} L' \overset{k_0}{\longrightarrow} L_D \overset{k_1}{\longrightarrow} L_O \overset{k_2}{\longrightarrow} L_E \overset{K_3}{\rightleftharpoons} L_A \quad (25)$$

taking into account two desorption equilibria

$$L_D \overset{K_{D1}}{\rightleftharpoons} L_{D1} \quad (26)$$

$$L_O \overset{K_{D2}}{\rightleftharpoons} L_{O1} \quad (27)$$

where L_{D1} into L_{O1} are the species L_D into L_O dissolved in water. A formal kinetic analysis of the reaction system in eqs 25−27 yields the following equation

$$Y = A_0 + A_1\left(1 - \exp\left(-\frac{k_1t}{1 + K_{D1}}\right)\right) + A_2\left(1 - \exp\left(-\frac{k_2t}{1 + K_{D2}}\right)\right) \quad (28)$$

Temperature variation will have the same effect on the activation energies as discussed for eq 22, bearing in mind that the constants K_{D1} and K_{D2} are *de*sorption constants. In fact, the models formulated with the reaction in eq 5 and that formulated with the reactions in eqs 25−27 are describing essentially the same situation, only in different terms. In both cases, adsorption/desorption equilibria are coupled to irreversible reactions leading to the complete opening and spreading of a liposome on a mercury electrode. This analysis of the formal kinetics of both models supports the interpretation of the experiments.

Conclusions

The present study shows that the adhesion of liposomes on mercury electrodes can be modeled as a three-step process, where the first step consists of a fast and weak equilibrium of adsorption of intact liposomes, followed by an irreversible docking by adsorption of one or some lecithin molecules of the liposome. The second step consists of the opening of the liposome and the adsorption of the opened liposome, and the third step consists of the spreading of a lecithin layer and its adsorption on the mercury surface. The empirical eq 3 agrees very well with eq 22 derived from a formal kinetic analysis of the mechanism depicted in Figure 10 and described by the reaction sequence in eq 5. The resulting model is in very good agreement with models published to understand the spreading of lipsomes at the solution−gas interface,[40,45] and it is consistent with models used to explain the fusion of liposomes.[46] The methodology described in this paper is presently being used to study the effects of foreign molecules incorporated in liposome membranes on the stability of the membranes.

Acknowledgment. D.H. thanks the Lipoid GmbH for provision of a scholarship and supply of lecithins. V.A.H. acknowledges provision of a DAAD Conacyt scholarship. F.S. acknowledges Fonds der Chemischen Industrie for financial support.

References and Notes

(1) Van de Vosseberg, J. L. C. M.; Driessen, A. J. M.; da Costa, M. S.; Konings, W. N. *Biochim. Acta* **1999**, *97*, 1419.
(2) Heerklotz, H.; Seelig, J. *Biophys. J.* **2002**, *82*, 1445.
(3) Grabitz, P.; Ivanova, V. P.; Heimburg, T. *Biophys. J.* **2002**, *82*, 299.
(4) Ivanova, V. P.; Heimburg, T. *Phys. Rev. E* **2001**, *63*, 041914.
(5) Dimova, R.; Pouligny, B.; Dietrich, C. *Biophys. J.* **2002**, *79*, 340.
(6) Bagatolli, L. A.; Gratton, E. *Biophys. J.* **1999**, *77*, 2090.
(7) Bagatolli, L. A.; Gratton, E. *Biophys. J.* **2000**, *78*, 290.
(8) Bagatolli, L. A.; Gratton, E. *Biophys. J.* **2000**, *79*, 434.
(9) Bagatolli, L. A.; Parasassi, T.; Gratton, E. *Chem. Phys. Lipids* **2000**, *105*, 135.
(10) Bagatolli, L. A. *Chem. Phys. Lipids* **2003**, *122*, 137.
(11) Brumm, T.; Jørgensen, K.; Mouritsen, O. G.; Bayerl, T. M. *Biophys. J.* **1996**, *70*, 1373.
(12) Miller, I. R.; Bach, D. *J. Colloid Interface Sci.* **1968**, *20*, 250.
(13) Miller, I. R.; Blank, M. *J. Colloid Interface Sci.* **1968**, *26*, 34.
(14) Pagano, R. E.; Miller, I. R. *J. Colloid Interface Sci.* **1973**, *45*, 126.
(15) Miller, I. R.; Rishpon, J.; Tenenbaum, A. *Bioelectrochem. Bioenerg.* **1976**, *3*, 528.
(16) Miller, I. R.; Yavin, E. *Bioelectrochem. Bioenerg.* **1988**, *19*, 557.
(17) Miller, I. R.; Vinkler, H. *Bioelectrochem. Bioenerg.* **1989**, *22*, 365.
(18) Miller, I. R.; Doll, L. *Bioelectrochem. Bioenerg.* **1990**, *24*, 129.
(19) Nelson, A.; Benton, A. *J. Electroanal. Chem.* **1986**, *202*, 253.
(20) Nelson, A.; Auffret, N. *J. Electroanal. Chem.* **1988**, *244*, 99.
(21) Nelson, A.; Auffret, N. *J. Electroanal. Chem.* **1988**, *248*, 167.

(22) Nelson, A.; van Leeuwen, H. P. *J. Electroanal. Chem.* **1989**, *273*, 183.
(23) Rueda, M.; Navarro, I.; Ramirez, G.; Prieto, F.; Nelson, A. *J. Electroanal. Chem.* **1998**, *454*, 155.
(24) Monelli, M. R.; Guidelli, R. *J. Electroanal. Chem.* **1992**, *326*, 331.
(25) Becucci, L.; Monelli, M. R.; Guidelli, R. *J. Electroanal. Chem.* **1996**, *413*, 187.
(26) Buoninsegni, F. T.; Becucci, L.; Monelli, M. R.; Guidelli, R. *J. Electroanal. Chem.* **2001**, *500*, 395.
(27) Guidelli, R.; Aloisi, G.; Becucci, L.; Dolfi, A.; Monelli, M. R.; Buoninsegni, F. *J. Electroanal. Chem.* **2001**, *504*, 1.
(28) Stauffer, V.; Stoodley, R.; Agak, J. O.; Bizzotto, D. *J. Electroanal. Chem.* **2001**, *516*, 73.
(29) Shepherd, J.; Yang, Y.; Bizzotto, D. *J. Electroanal. Chem.* **2002**, *524*−*525*, 54.
(30) Stoodley, R.; Bizzotto, D. *Analyst* **2003**, *128*, 552.
(31) Bizzotto, D.; Nelson, A. *Langmuir* **1998**, *14*, 6269.
(32) Žutić, V.; Kovač, S.; Tomaič, J.; Svetličić, V. *J. Electroanal. Chem.* **1993**, *349*, 173.
(33) Ivošević, N.; Tomaič, J.; Žutić, V. *Langmuir* **1994**, *10*, 2415.
(34) Kovač, S.; Svetličić, V.; Žutić, V. *Colloids Surf., A* **1999**, *149*, 481.
(35) Ivošević, N.; Žutić, V.; Tomaič, J. *Langmuir* **1999**, *15*, 7063.
(36) Svetličić, V.; Ivošević, N.; Kovač, S.; Žutić, V. *Bioelectromagnetics* **2000**, *53*, 79.
(37) Hozić, A.; Svetličić, V. *Electrophoresis* **2002**, *23*, 2080.
(38) Hellberg, D.; Scholz, F.; Schauer, F.; Weitschies, W. *Electrochem. Commun.* **2002**, *4*, 305.
(39) Scholz, F.; Hellberg, D.; Harnisch, F.; Hummel, A.; Hasse, U. *Electrochem. Commun.* **2004**, *6*, 929.
(40) Li, M.; Retter, U.; Lipkowski, J. *Langmuir* **2005**, *21*, 4356.
(41) Designed by Dario Omanović, Rudjer Boskovic Institute, Zagreb, Croatia (E-mail: omanovic@irb.hr).
(42) Lagüe, P.; Zuckermann, M. J.; Roux, B. *Biophys. J.* **2001**, *81*, 276.
(43) Agak, J. O.; Stoodley, R.; Retter, U.; Bizzotto, D. *J. Electroanal. Chem.* **2004**, *562*, 135.
(44) Press, W. H.; Flannery, B. P.; Teukolsky, S. A.; Vetterling, W. T. *Numerical Recipes in Pascal*; Cambridge University Press, Cambridge, U.K., 1992; pp 551 and 586.
(45) Mitev, D. J.; Ivanova, Tz.; Vassilieff, C. S. *Colloids Surf., B* **2002**, *24*, 185.
(46) Lee, J. K.; Lentz, B. R. *Proc. Natl. Acad. Sci. U.S.A.* **1998**, *95*, 9274.